Exergetic, economic and carbon emission studies of bio-olefin production via indirect steam gasification process

Peng Jiang, Ashak Mahmud Parvez, Yang Meng, Meng-xia Xu, Tian-chi Shui, Cheng-gong Sun, Tao Wu

University of Nottingham Ningbo China, 199 Taikang East Road, Ningbo, 315100, China

First published 2019

University of Nottingham
UK | CHINA | MALAYSIA

Exergetic, economic and carbon emission studies of bio-olefin production via indirect steam gasification process

Peng Jiang [a], Ashak Mahmud Parvez [b], Yang Meng [a], Meng-xia Xu [a], Tian-chi Shui [c], Cheng-gong Sun[d], Tao Wu [a*]

[a] *Key Laboratory of Clean Energy Conversion Technologies, The University of Nottingham Ningbo China, Ningbo 315100, PR China*

[b] *Department of Mechanical Engineering, University of New Brunswick, 15 Dineen Drive, Fredericton NB E3B 5A3, Canada*

[c] *Department of Architecture and Built Environment, The University of Nottingham Ningbo China, Ningbo 315100, PR China*

[d] *Department of Chemical and Environmental Engineering, The University of Nottingham, NG7 2RD, UK*

[*]Corresponding author. *Email address:* Tao.Wu@nottingham.edu.cn

ABSTRACT

The indirect steam gasification of biomass to olefins (IDBTO) coupled with CO_2 utilization was proposed and simulated. Energy and exergy efficiencies, net CO_2 emissions, and economic evaluation were performed against IDBTO as well as the direct oxygen-steam gasification of biomass to olifins (DBTO). The influences of unreacted gas recycling fraction (RU) and CO_2 to dry biomass mass ratio (CO_2/B) on the thermodynamic performance of the processes were also studied. The results showed that the yields of olefins of DBTO and IDBTO were 17 wt% and 19 wt%, respectively, the overall energy and exergy efficiencies of the IDBTO were around 49% and 44%, which were 8% and 7% higher than those of the DBTO process, respectively. A higher RU was found favor higher energy and exergy efficiencies for both routes. Besides, for the IDBTO process, it is found that the addition of CO_2 to gasification system led to an improvement in both energy efficiency and exergy efficiency by around 1.6%. Moreover, life-cycle net CO_2 emission was predicted to be -4.4 kg CO_2 eq./ kg olefins for IDBTO, while for DBTO, it was -8.7 kg CO_2 eq./ kg. However, the quantitative economic performance of IDBTO was superior to that of the DBTO process.

Key words: Bio-olefin; Thermodynamic analysis; Environmental assessment; CO_2 utilization; Negative net CO_2 emission; Techno-economic analysis

1. Introduction

Light olefins including ethylene and propylene are the most important petrochemicals [1], and have been widely used in the production of plastics, elastomers and rubbers [2]. At present, the production of olefins relies on the thermal steam cracking of naphtha. However, the growing demand in olefins together with the depletion and unsustainable nature of petroleum supply [3] have made it imperative to develop alternative routes for the synthesis of olefins.

Methanol to olefins (MTO) offers a financially feasible pathway to utilize other types of fossil fuels, such as coal and natural gas for the production of olefins [4]. Because of the energy mix of China, which is rich in coal and short in oil, many attempts have been made to develop processes for the conversion of coal to olefins (CTO). In 2010, the world first commercial MTO plant with an olefin production rate of 600 kt/y was launched in Shenhua, China. It is projected that the production of olefins from methanol will reach 15 Mt/y in 2020 [5], which accounts for about 20% of the total olefin production in China. However, a well-to-wheel analysis showed that the greenhouse gas emissions (GHG) from CTO was 2.6 times higher than that of the oil to olefins (OTO) process, while after a carbon capture unit was added, the GHG emission would still be 1.7 times of the OTO process [6]. Apart from GHG emission, the H_2/CO molar ratio in syngas from coal gasification is usually in the range of 0.2 to 1, which is not appropriate for the synthesis of methanol [7]. Thus, the CTO process requires a large quantity of steam in order to adjust the H_2/CO ratio to be around 2.05 to 2.1.

Biomass is considered as an inherently carbon-neutral renewable resource, which contains more hydrogen than coal [8]. Therefore, the employment of biomass as the raw material for the production of olefins is regarded as a sustainable decarbonization approach. This scheme can be implemented through

biomass gasification to methanol followed by the conversion of methanol to olefins. Basically, there are two types of gasification technologies: indirect gasification and direct gasification [9]. Indirect gasification uses steam as the gasifying medium and the heat is provided by a combustor while both oxygen and steam are employed for the direct gasification. Concerning biomass to olefins, most studies were focused on the use of direct biomass gasification as the syngas production unit [2, 10-12]. Hannula et al. developed a biomass to olefins process via methanol as the platform product and the syngas was generated by using a fluidized-bed steam/O_2 gasifier [2]. Lately, a life cycle assessment of biomass to ethylene process with gasification and fermentation routes, separately, showed that the gasification route had lower impact to the environment [10]. The comparison on olefins production through methanol or DME as the platform chemicals based on entrained biomass gasification indicated that no significant thermodynamic differences could be identified for these two cases [12]. In addition, comparative techno-economic analyses of oil-to-olefins, coal-to-olefins with or without carbon capture were investigated [3, 13-15]. However, very limited studies have been reported on the utilization of the indirect steam gasification of biomass as a source of syngas for the synthesis of olefins through methanol as the intermediate. Besides, the consideration of CO_2 as a gasifying agent for the enhancement of olefins' production has not been reported. The quantitative evaluation of life cycle CO_2 emission and economic analysis from biomass to olefins are also scarce.

In this study, a conversion of biomass to olefins via the indirect steam gasification of biomass coupled with CO_2 utilization process was proposed and simulated using Aspen Plus^{TM}. Moreover, the performance of the proposed route was evaluated in terms of olefins yield, energy and exergy efficiencies, followed by a systematic comparison with the synthesis of olefins via the direct oxygen-steam gasification of biomass. The effects of some important parameters, such as unreacted gas recycling fraction and CO_2 to dry biomass mass ratio, on the thermodynamic performance were also discussed.

Finally, life cycle CO_2 emission and economic evaluations of these two cases were performed in this work.

2. Process description and simulation

The schematic diagrams of the DBTO and IDBTO are shown in Fig.1 (a) and Fig.1 (b), respectively. The production of olefins using biomass as feedstock mainly consists of three parts, namely, bio-syngas generation, methanol synthesis and purification, olefins synthesis and separation. The main difference between the two processes lies in the syngas generation strategy. As shown in Fig. 1, the DBTO process uses steam and O_2 as the gasifying agents, in which biomass is gasified in a pressurized fluidized-bed reactor combined with a catalytic reforming unit to convert the long carbon chain hydrocarbons into syngas, while the IDBTO process comprises a biomass steam gasifier interconnected with a combustor providing heat that is required by the gasification system. The outlet gas composition from the biomass steam gasifier contains less heavy hydrocarbons due to the use of steam [16]. Besides, a suitable H_2/CO ratio for methanol synthesis is controlled by the addition of an appropriate amount of CO_2, which is readily from acid gas removal unit (AGR), as the gasifying agent. Methanol is produced and purified in the methanol synthesis and purification subsystems. Olefins synthesis and separation subsystems utilize methanol to produce olefins in a DMTO reactor and separate the olefins mixture into polymer-grade ethylene and propylene. Detailed descriptions of the subsystems and simulations are illustrated in the following sections.

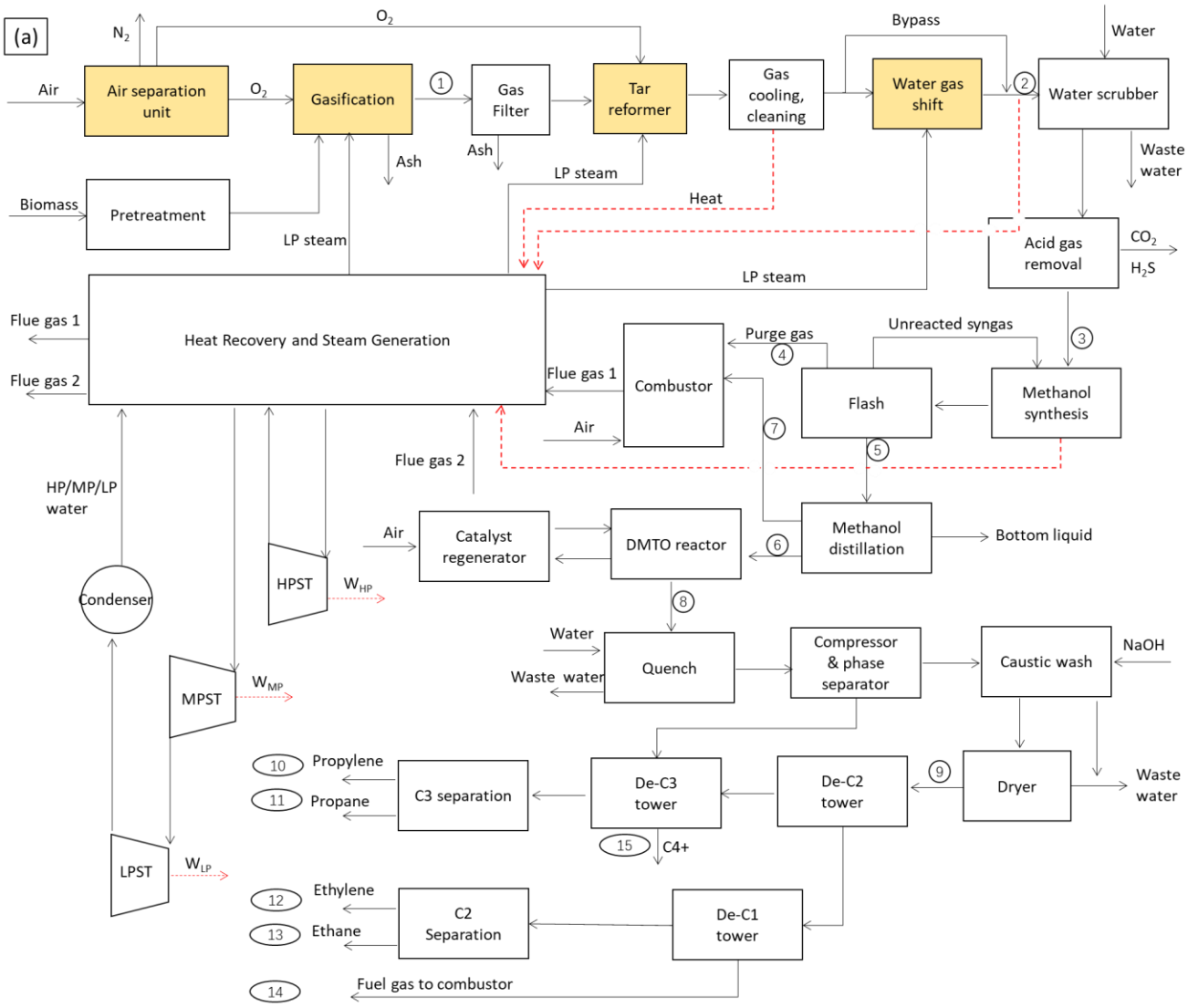
(a)
N2
O2
Air
Air separation unit
O2
Gasification
1
Gas Filter
Tar reformer
Gas cooling, cleaning
Bypass
Water gas shift
2
Water
Water scrubber
Waste water
Ash
Ash
LP steam
Heat
Biomass
Pretreatment
LP steam
Acid gas removal
CO2
H2S
LP steam
Flue gas 1
Heat Recovery and Steam Generation
Flue gas 2
Purge gas
4
Unreacted syngas
3
Flue gas 1
Combustor
Air
Flash
Methanol synthesis
7
5
Flue gas 2
HP/MP/LP water
Air
Catalyst regenerator
DMTO reactor
6
Methanol distillation
Bottom liquid
Condenser
HPST
WHP
8
Water
Waste water
Quench
Compressor & phase separator
Caustic wash
NaOH
MPST
WMP
10
Propylene
11
Propane
C3 separation
De-C3 tower
De-C2 tower
9
Dryer
Waste water
15
C4+
LPST
WLP
12
Ethylene
13
Ethane
C2 Separation
De-C1 tower
14
Fuel gas to combustor

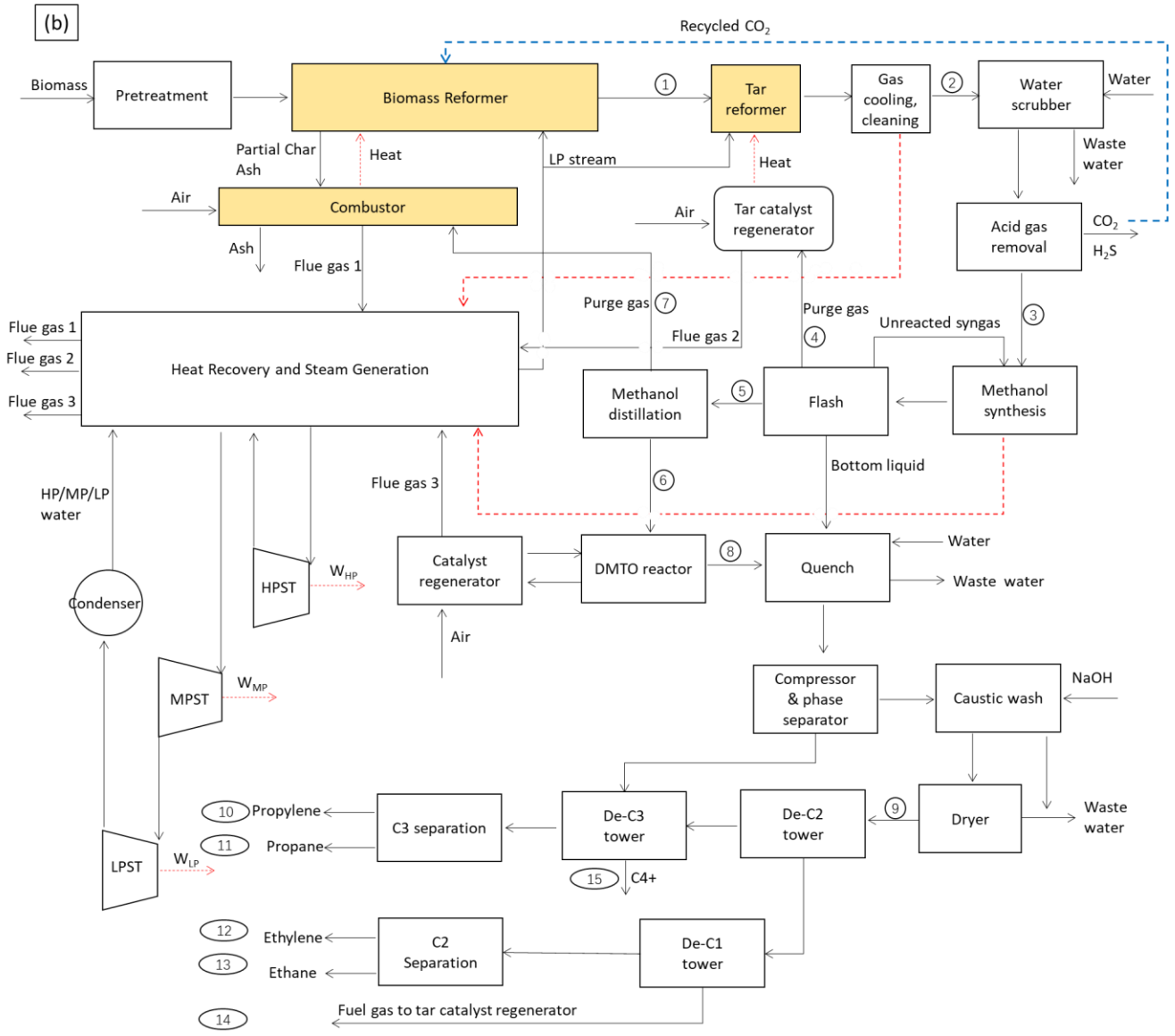

Fig.1. Schematic diagram of the biomass to olefins process based on: (a) DBTO; (b) IDBTO

2.1. Bio-syngas generation

The feedstock considered in this study was wood chip. The ultimate and proximate analysis data are listed in Table 1 [17]. In the DBTO process, the dried wood chips were fed into the fluidized-bed gasifier at an elevated pressure of 0.5 MPa via a lock-hopper. The gasification medium (a mixture of steam and oxygen) was injected to realize the conversion of fuel into CO, H_2, CO_2, CH_4, and a small portion of heavier hydrocarbons and tars. The use of oxygen made it possible to avoid nitrogen dilution and also

had the advantage of auto-thermal operation [18]. The raw syngas generated from gasifier after particulate matter removal in a hot gas filter was sent to an autothermal tar reforming unit, in which most of the tar and high hydrocarbons were catalytically cracked into CO and H_2 at a temperature of approximately 860 ^oC [19, 20]. After that, the syngas was cooled and fed into a wet scrubber and a sulfur removal reactor (a ZnO bed) to eliminate other particles and sulphur. The clean syngas was partly directed to an adiabatic water gas shift reactor (WGSR) to reach the desired H_2/CO ratio in the range of 2.05-2.1 for the methanol synthesis [11, 21]. The waste heat was recovered in the heat recovery and steam generation (HRSG) unit.

Table 1 Ultimate and proximate analysis of the wood chip.

Ultimate analysis (wt%, dry basis)		Proximate analysis (wt %)	
C	50.7	Moisture	6.9
H	6.2	Volatile	83.3
N	0.1	Fixed carbon	16.5
S	0.01	Ash	0.2
O (by difference)	42.8	HHV(MJ/kg)	20.6

The simulation strategy for the direct gasification of biomass was adopted from the concept detailed elsewhere [17, 22]. The RYield and RGibbs modules were employed to simulate biomass decomposition and gasification, respectively [23]. The tar (*i.e.*, $C_{10}H_8$) catalytic reforming unit was modelled using a RGibbs module, the conversions of hydrocarbon were adjusted according to other researchers' work [24, 25]. For the simulation of WGS reaction, a temperature approach of 10 ^oC was considered in the REquil model [26]. The simulated wet syngas compositions from the gasifier in comparison with the experimental data are presented in Fig.2 (a). It is confirmed that the simulation values agree well with the experimental data, indicating that accuracy of the model is acceptable.

However, for the proposed scheme in Fig. 1(b), the biomass steam gasification took place in a dual fluidized-bed reactor. The heat for endothermic gasification reactions was supplied by the combustion of char and the purge gas from methanol distillation. Sand was circulated as the heat carrier between the biomass reformer and combustor via a loop seal [27]. The biomass steam reforming could produce hydrogen-rich syngas without being diluted by nitrogen [28]. Typically, at the gasification temperature about 850 ^{o}C and steam to biomass mass ratio (STBR) of 0.75, the syngas from the gasifier produced a H_2/CO ratio of 2.3. However, by adding CO_2 as a gasifying agent, the H_2/CO ratio at the outlet of the tar reformer could be adjusted to 2.05-2.1, suiting for the synthesis of methanol [29]. This aspect is discussed extensively in Section 4.3. The raw syngas was routed to a catalytic tar cracker, which comprised of a reformer and a catalyst regenerator. In the reformer, hydrocarbons and tars reacted with steam to produce syngas in the presence of a catalyst (Ni/Mg/K supported by Al_2O_3) [30]. The spent catalyst was regenerated in the tar catalyst regenerator. Heat for the tar reformer was provided by the combustion of the purge gas from methanol flash unit along with fuel gas from De-C1 tower in the regenerator. As can be seen from Fig.1, compared with the DBTO process, the WGS and ASU systems were avoided in the IDBTO that will reduce total cost and shorten process route.

The simulation of the biomass indirect gasification was carried out by the Ryield and RGibbs modules [31, 32]. The combustor was simulated using a RGibbs block. The biomass steam gasifier temperature was kept lower than the combustor temperature by 50 ^{o}C to ensure sufficient heat transfer. The carbon conversion in the biomass gasifier was assumed to be 70% [33], and the residual char was directed to combustor. The biomass steam gasification model is validated by comparing the outlet syngas composition between literature data and simulation values, as shown in Fig. 2(b). As indicated, the deviation is less than 2%, which proves the validity of the model [34].

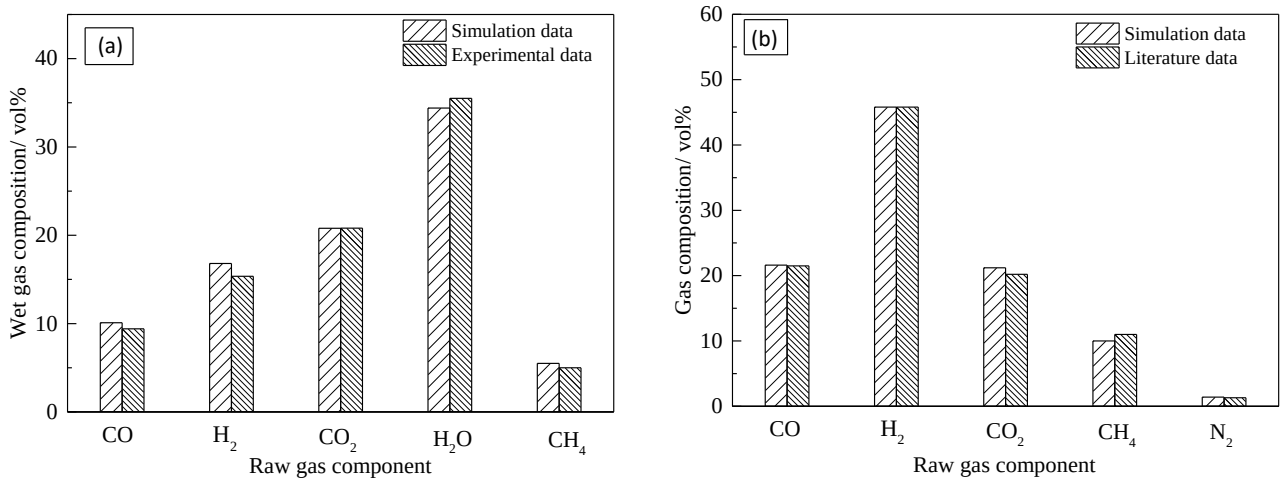

Fig.2. Comparison of the outlet syngas composition between simulation data and the experimental/literature data. (a) DBTO process, $T_{Gasifier}$=823 °C, STBR=0.5, and oxygen to fuel ratio of 0.31 [17]. (b) IDBTO process, $T_{Gasifier}$=850 °C and STBR=0.75 [34].

2.2. Methanol synthesis and purification

The syngas from WGSR or tar reformer was cooled down and scrubbed with water to remove particulate matters, ammonia and halides, etc. The clean syngas was then compressed to 2.0 MPa before it was decarbonized in the Rectisol-based unit. Approximately 90% of the CO_2 in the feed gas was removed to achieve the molar ratio of $(H_2-CO_2)/(CO_2+CO)$ = 2.03 and $H_2/(2CO+3CO_2)$ = 1 in the purified syngas [35, 36]. Then, the pure syngas was compressed to the desired operating pressure (8.0 MPa) and was introduced to methanol synthesis reactor, where methanol was synthetized over a commercial catalyst of $Cu/ZnO/Al_2O_3$. The main reactions for the synthesis of methanol are presented as [37]:

$$CO+2H_2 \rightarrow CH_3OH,\ \Delta H_{25°C} = -90.9kJ/mol \quad (1)$$

$$CO_2+3H_2 \rightarrow CH_3OH+H_2O,\ \Delta H_{25°C} = -50.1kJ/mol \quad (2)$$

The product gas was cooled down and the unreacted gas was separated from the raw methanol in the flash unit. Then, a large portion of unreacted gas was recycled to the methanol reactor to enhance the

methanol yield, while the remaining was purged to combustors. In this study, the Lurgi synthesis reactor was used and simulated using a REquil block with a temperature approach of 10 ^{o}C [38]. Raw methanol from the flash tank was purified through a stripper and a distillation columns [39], which were simulated via RadFrac blocks. To validate the methanol unit, the inlet syngas composition, temperature and pressure of the methanol reactor was taken from the reference [40]. The comparison of the product gas between the predicted value and literature value is shown in Table 2. It is clear that the model value agrees well with the literature data, demonstrating that the model was reliable and could be employed for the simulation.

Table 2 Comparison between the simulation value and literature value

Composition (mole %)	CO	H_2	CO_2	H_2O	CH_4O
Model predicted value	0.075	0.472	0.101	0.009	0.344
Literature value [40]	0.073	0.473	0.102	0.007	0.343

2.3. Olefins synthesis and separation

The methanol product from the top of methanol distillation tower was pumped and superheated before it was sent to the turbulent fluidized-bed MTO reactor. DMTO technology developed by Dalian Institute of Chemical Physics was considered in the olefins production unit due to its high methanol conversion (99.8%) and high ethene and propene selectivity (80%) [7]. SAPO-34 catalyst was used as the catalytic medium for the olefins production owing to its excellent catalytic performance and high thermal stability [41]. Deactivated catalyst due to coke formation was burned in the regenerator at 600 ^{o}C and recycled to the DMTO reactor, while the flue gas was routed to HRSG to recover heat. The main reactions that occurred in the reactor are shown as below [13, 42]:

$$2CH_3OH \rightarrow C_2H_4 + 2H_2O,\ \Delta H_{25^\circ C} = -23.1 kJ/mol \quad (3)$$

$$3CH_3OH \rightarrow C_3H_6 + 3H_2O,\ \Delta H_{25^\circ C} = -92.9 kJ/mol \quad (4)$$

$$4CH_3OH \rightarrow C_4H_8 + 4H_2O,\ \Delta H_{25^\circ C} = -150.0 kJ/mol \quad (5)$$

The effluent of the DMTO reactor was cooled down and introduced to the water-quench column. Afterwards, the vapor gas from the quench tower was compressed to 2.5 MPa and directed to the caustic wash tower for CO_2 removal. The remaining gas was fed to a molecular sieve dryer before it was sent to the downstream olefins separation units. The moisture-free gas was firstly fed into de-ethaniser (De-C2) to separate methane, ethylene, ethane and other light gases from propylene and other heavier components. The overhead light components were then injected into de-methaniser (De-C1) column where methane-rich fuel gas was separated from the mixture of ethane and ethylene. Subsequently, the overhead fuel gas was directly sent to combustion chamber. The bottom product from De-C1 was further distillated in the C2 separation column, in which polymer-grade ethylene component was obtained at the overhead stream [43]. The bottom stream from De-C2 was directed to the de-propaniser (De-C3) to split propylene and propane from heavy hydrocarbons such as butylene and pentane (C4+). To obtain polymer-grade propylene, the overhead product from De-C3 was sent to the C3 separation column to recover the propylene at the top. In this study, the desired olefins were ethylene and propylene.

DMTO reactor was operated at 490 ^oC and 0.22 MPa and was modelled by a RYield module [2] specifying the mass yield distribution of each component described elsewhere [44]. The catalytic regenerator was simulated using a RStoic reactor [2]. Water quench tower and olefins separation columns were simulated using the RadFrac block. Table 3 shows the main design parameters and assumptions during the simulation of the above two processes [13, 43, 45, 46].

Table 3 Simulation assumption and operation conditions for the main components.

Item	Operation conditions

Biomass	Mass rate: 5 kg/s
Air separation unit	Oxygen purity: 99 vol% Power consumption: 325 kWh/ton O_2 delivery pressure: 0.55 MPa
Pressurized steam /O_2 gasifier	Operating pressure: 0.5 MPa Oxygen to fuel mass ratio: 0.42 STBR: 0.54 Heat loss: 1% HHV of feeding biomass
Biomass steam gasifier and combustor	STBR: 0.75 CO_2 to biomass mass ratio: 0.143 Operating pressure: 0.15 MPa Air excess molar ratio in combustor: 1.2
Tar reformer (IDBTO process)	Mole conversion : CH_4=80%; C_2H_6=99%;C_2H_4=90% $C_{10}H_8$=99.9%; C_6H_6=99%;NH_3=90%
Water gas shift reactor	Steam to CO molar ratio: 2 Equilibrium temperature approach: 10 ^oC Operation pressure: 0.4 MPa
Acid gas removal	Rectisol CO_2 removal CO_2 molar fraction after absorption: 3% Refrigeration work: 0.55 kWh/kmol CO_2 removed Utility electricity: 0.53 kWh/kmol CO_2 removed
Methanol synthesis reactor	Temperature: 260 ^oC Pressure: 8.0 MPa
Methanol separation	Stripper column: 10 stages; reflux ratio: 1.6, B/F=0.91; operating pressure: 0.45 MPa

	Methanol distillation column: 30 stages; total condenser; reflux ratio:0.73; D/F=0.964;operating pressure: 0.4 MPa; methanol purity: > 99.5% (wt)
Olefins separation	Ethylene molar purity: 99.9% Propylene molar purity: 99% Cooling work consumption: 62 kJ/kg methanol
Purge gas/Fuel gas combustor	Combustion temperature 950 °C
Heat recovery steam generation	High pressure steam (HP): 12.0 MPa Medium pressure steam (MP): 3.4 MPa Low pressure steam (LP): 0.6 MPa Condenser pressure: 0.005 MPa Reheated temperature: 540 °C
Compressors and steam turbines (ST)	Isotropic efficiency: 0.88 Mechanical efficiency: 0.99

3. Performance analysis methodology

3.1. Thermodynamic evaluation

Thermodynamic evaluation of both olefins production processes was conducted with a focus on energy and exergy analyses. Energy efficiency tracks the efficiency of converting biomass to olefins and power, which is defined as:

$$\eta_{en} = \frac{W_{net} + LHV_{olefins} \times \sum m_{olefins}}{m_{bio} \times LHV_{bio}} \quad (6)$$

where $m_{olefins}$ and m_{bio} represent the mass flow rate of the olefins product and the biomass feedstock, respectively. Here, *LHV* represents the lower heating value and W_{net} is the net power output.

Exergy follows the conservation of Second Law of Thermodynamics and for a system and is expressed by [47]:

$$\sum E_{x,in} = \sum E_{x,out} + \sum E_{x,des/loss} \quad (7)$$

where $\sum E_{x,in}$ and $\sum E_{x,out}$ are the total exergy input into a system and output from a system including the material stream and heat stream, respectively. $\sum E_{x,des/loss}$ is a combination term of exergy destruction and loss owing to the irreversibility of a system and streams exited to the environment from a system without further utilization, respectively [47].

The exergy efficiency of the overall system is defined as:

$$\eta_{ex} = \frac{W_{net} + \sum E_{x,olefins}}{E_{x,bio}} \quad (8)$$

where $\sum E_{x,olefins}$ is the olefins exergy output and $E_{x,bio}$ stands for the chemical exergy of biomass.

$E_{x,bio}$ can be deduced according to the common exergy formula (O/C mass ratio ≤2) as follows [48]:

$$E_{x,bio} = \beta m_{\text{bio}} \cdot \text{LHV}_{\text{bio}} \quad (9)$$

$$\beta = \frac{1.044 + 0.016\frac{h}{c} - 0.3496\frac{o}{c}\left(1 + 0.0531\frac{h}{c}\right) + 0.0493\frac{n}{c}}{1 - 0.4124\frac{o}{c}} \quad (10)$$

where h, c, o, n stand for the mass fraction of H, C, O, N in the ultimate analysis of biomass, respectively.

3.2. Environmental evaluation

Life cycle analysis (LCA) enables the identification and evaluation of environmental burdens of the biomass to olefins production from cradle-to-gate perspective [10]. The conduction of LCA analysis usually involves four components, namely, objective and boundary definition, inventory data collection, environmental assessment, and interpretation of the results. Fig.3 shows the boundary of the biomass to olefins processes. The main units inside the boundary are biomass production, collection and transportation, pretreatment, syngas production either using the direct gasification or indirect gasification subsystem, methanol synthesis and rectification, olefins synthesis and separation, combustion of char, purge gas and fuel gas, HRSG and steam turbines. The main emissions were CO_2, NO_x, SO_2, waste water

and waste solids, which are associated with a series of environmental effects, such as abiotic depletion, acidification, human toxicity, eutrophication and photochemical oxidation. In this study, CO_2 emission equivalent was used to compare environmental behaviors of these two processes [49].

The CO_2 emission included two major sources, direct emission and indirect emission. Indirect CO_2 emission consisted of the CO_2 emission from biomass production, transportation and pretreatment. On the contrary, direct CO_2 emission originated from the combustion system fueled by purge gas, char and fuel gas. The CO_2 emission from biomass production was calculated to be 133.03 kg equivalent CO_2 per ton while for biomass pretreatment, the value was 7.46 kg CO_2 eq./ ton [50]. The CO_2 emission from biomass transport was assumed to be 1504 kg CO_2/km, which was a typical CO_2 emission rate for a diesel-fueled heavy vehicle (capacity: 10 t) [51]. In addition, landfill of ash and uncovered carbon was also considered. Generally, the CO_2 emissions from plant construction, manufacture of materials, maintenance and plant dismantling should be considered. However, due to their less significant contribution [49], they were not included in this study. The direct CO_2 emissions were counted directly from the simulation results.

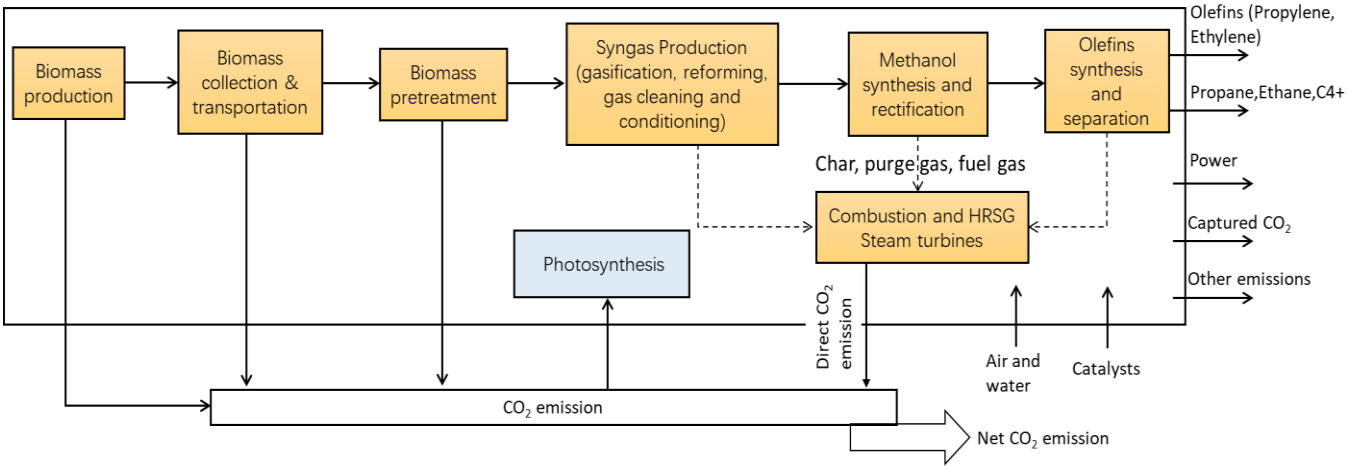

Fig.3. System boundary considered for life cycle evaluation.

3.3. Economic evaluation

This work employed the total capital costs, net present value (NPV) and internal rate of return (IRR) to justify the economic feasibility of the proposed process. The total capital cost was estimated by direct and indirect capital costs based on the ratio factor method outlined in literature [52, 53]. The estimation of individual equipment is determined by the base equipment cost and size [54].

$$C_{eqB} = C_{eqA}\left(\frac{Q_B}{Q_A}\right)^{SF} \quad (11)$$

where *SF* is scaling factor ranging from 0.5 to 1. Here, C_{eqB} and Q_B are the predicted equipment cost and size, respectively. The terms of C_{eqA} and Q_A are the reference equipment cost and size, which are obtained from literature [13, 52, 55-59] and are summarized in Table 4. In addition, the installation and control, construction phase, land, site preparation, plant start-up and contingency costs, were further calculated based on the ratio factors of the total equipment cost referred in [52, 53].

Table 4 Investment costs estimates for the main components.

Units	C_{eqA}	Q_A(M$,2016)	SF	Reference
Biomass pretreatment	17.9 kg/s as received biomass	4.29	0.77	[55]
ASU	6.67 kg-O_2/s	21.9	0.75	[52]
Direct gasification subsystem (incl. auto-thermal tar reforming and scrubbing)	17.9 kg/s dry biomass	54.34	0.77	[56]
Indirect gasification subsystem (incl. steam tar reforming and scrubbing)	23.1 kg/s dry biomass	33.58	0.77	[57]
WGS	150 kg/s feed gas	3.47	0.67	[58]
AGR	2064.4 mol/s CO_2 captured	30.39	0.67	[13]

Methanol synthesis and separation	35.647 kg/s feed	7.61	0.65	[58]
MTO	62.5 kg methanol /s	206.7	1	[13]
HRSG	355 MW_{th} boiler duty	53.61	1	[59]
Steam cycle and power generation	275 MW_e ST gross power	68.77	0.67	[59]

Fixed operating cost was estimated according to the percentages of total indirect cost (TIC) or personnel cost [53]. Here, the cost of personnel is calculated based on the total LHV of biomass [52, 57]:

$$C_{Personnel} = 0.67M\$/100MW_{LHV} \quad (12)$$

Variable operating costs, such as water and catalyst and ash disposals, were calculated based on their prices and consumable rates. However, the total cost of biomass was estimated by the consideration of production, collecting, storage and road transportation cost, and the former three were 22.1, 11.7, 3.7 $/tonne dry biomass respectively [60, 61]. The road transportation cost is dependent on biomass collection distance, which is also determined by the plant size. The expressions for the estimation of costs were adopted from the literature [61, 62]. Biomass land coverage was set as 10% to ensure the biomass supply.

The NPV was used to identify the present sum of net cash flow over an entire plant life. To calculate NPV, the net earnings at years *t* should be discounted to year zero with a Marginal Rate of Return [63]. The expression for NPV is presented as [15]:

$$\text{NPV} = \sum_{t=-1}^{n} \frac{CF_t}{(1+i)^t} \quad (13)$$

where CF_t represents the cash flow in year *t*. The range of *t* is from -1 to 20, which stands for the construction time of 2 years and plant life span of 20 years. Table 5 shows the main parameters and assumptions for the economic evaluation [64-66].

The IRR is another parameter to measure the profitability of a potential project [67]. It discounts all the cash flow back into year zero and leads to the *NPV* equaling to zero. When IRR$\geqslant i$, the project is profitable and a higher IRR means a better economy performance. The calculation of IRR is implemented as NPV=0 [37].

Table 5 Main parameters and assumption for economic evaluation [64-66].

Parameters	Value
Biomass price, $/ tonne dry	41.2
Water cost, $/ tonne	0.05
Electricity, $/ kWh	0.07
Catalyst and ash disposal cost, % of variable cost	2
Discount rate, %	8
Construction time, yr	2 (25%, 75%)
Personnel	Seeing Eqs.(12)
Depreciation	10 years, straight-line depreciation
	Salvage value: 5% of equipment costs
Tax rate (φ), %	20
Annual operation time, hr	8000
Ethylene, $/tonne	1300
Propylene, $/tonne	1400
Light paraffin (C1-C3), $/tonne	543
Mixture of C4+, $/tonne	672

4. Results and Discussion

In the biomass to olefins processes, the unreacted syngas recycling flow rate in the methanol synthesis unit was a crucial parameter to determine the overall performance. An insufficient unreacted syngas recycling flow rate leads to a low yield of intermediate (methanol), significantly affecting the performances (such as olefins yield, energy and exergy efficiencies as well as profitability) of the downstream process. The unreacted gas recycle fraction (RU) is defined:

$$\mathrm{RU} = \frac{\text{unreacted syngas back to the methanol reactor (molar basis)}}{\text{vapor flow rate from the flash unit after the methonal reactor (molar basis)}} \quad (14)$$

On the other hand, for IDBTO process, the employment of readily CO_2 from AGR unit as a gasifying agent could reinforce the gasification of biomass (especially the Boudouard reaction: $C+CO_2 \rightarrow 2CO$, $\Delta H_{25^\circ C}$ = 172 kJ/mol) so as to offer a carbon source to enhance the CO fraction in the output syngas, leading to a possibility to reach the suitable syngas production for downstream methanol application. Therefore, the injection flow rate of CO_2 into gasifier (denoted as CO_2 to dry biomass mass ratio, CO_2/B) had also influence on the methanol and olefins yield, resulting in different thermodynamic and economic performances.

4.1. Mass balance

The simulation results of the key nodes in the DBTO and IDBTO processes are presented in Table 6 and Table 7 respectively. Fig.4 shows the methanol, ethylene and propylene yields of the DBTO and IDBTO processes. Clearly in Fig.4, the mass yield of methanol in the DBTO is 51.1wt%, while that of the IDBTO is 57.5wt%. With respect to ethylene and propylene yield, for the IDBTO, it is 9.6wt% and 9.5 wt% while those for the DBTO are 8.5wt% and 8.4wt%, respectively. Clearly in Table 6, the syngas for methanol synthesis in the DBTO was less than that in the IDBTO (12186.6 kg/h, seeing Node3 in Table 7) mainly due to the combustion of partial syngas with oxygen in both autothermal gasifier and tar

reformer in the DBTO. As a consequence, the methanol production of higher quality in the IDBTO was expected, leading to a higher olefins yield for the IDBTO process.

In addition, owing to a similar process configuration of biomass to olefins between the DBTO and the previously published works [2, 45], comparisons of the methanol and olefins yields were conducted. It was found that both the calculated methanol and olefins yields of the DBTO were consistent with the respective methanol and light olefins yields of 51.08% and 16.93% reported by Hannula [2]. Meanwhile, Johansson also demonstrated that the methanol yield was 51.5% and the olefins yield was between 17.6% and 18.2% [45], suggesting that the proposed IDBTO process with an olefins yield of 19.1% was an attractive approach for bio-olefins production.

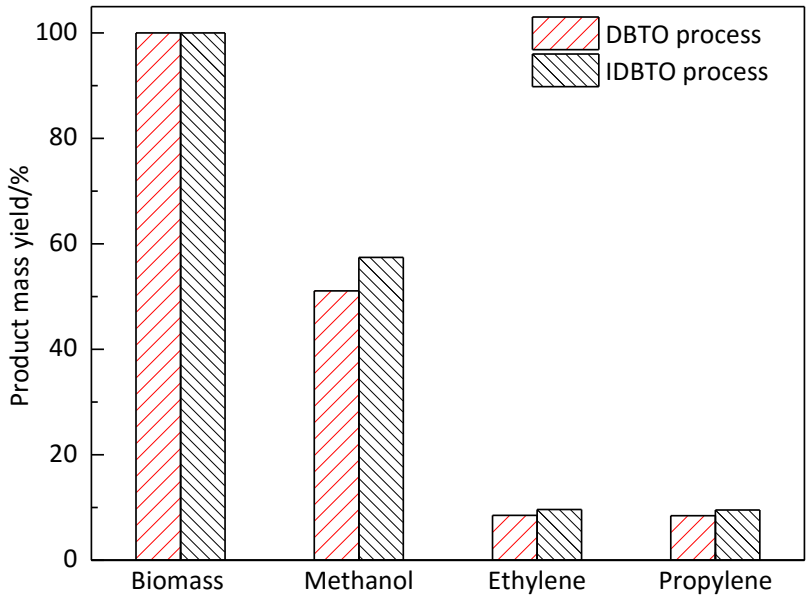

Fig.4. Comparison of mass yield of product between the DBTO and the IDBTO

Table 6 Simulation results for the main nodes shown in the DBTO process.

Node	T/°C	P/bar	Mass flow/(kg/h)	Mole fraction											
				CO	CO_2	H_2	H_2O	CH_4	C_2H_4	C_2H_6	C_3H_6	C_3H_8	C_4H_8	C_5H_{10}	Methanol
1	846.1	0.5	30368.2	0.14	0.23	0.20	0.35	0.06	0.02	0.01					
2	60	0.48	40958.2	0.13	0.21	0.28	0.38	0.01							
3	196	8	10374.7	0.30	0.04	0.64	0.00	0.02							
4	29.2	7.5	656.2	0.14	0.14	0.26		0.41							0.01
5	29.2	7.5	9713.3		0.06		0.05	0.02							0.88
6	87.5	0.3	8561.4												0.996
7	24.9	0.15	893.6	0.01	0.67	0.01		0.2							0.1
8	111	0.22	8445.7			0.06	0.68	0.01	0.13		0.09	0.01	0.02		
9	15	2.5	3563.5			0.2		0.02	0.42	0.01	0.27	0.02	0.05	0.01	
10	46.9	2	1415.5						0.01		0.99				
11	56	2	103.3								0.11	0.87	0.02		
12	-13.6	3	1425.2						0.999						
13	-5.5	3	61.18						0.58	0.42					
14	-91	3.05	95.6	0.01		0.91		0.07	0.01						
15	110.8	2.1	507.8								0.04	0.01	0.76	0.16	

Table 7 Simulation results for the main nodes shown in the IDBTO process.

Node	T/°C	P/bar	Mass flow/(kg/h)	Mole fraction											
				CO	CO_2	H_2	H_2O	CH_4	C_2H_4	C_2H_6	C_3H_6	C_3H_8	C_4H_8	C_5H_{10}	Methanol
1	831.8	0.15	26348.1	0.18	0.15	0.36	0.27	0.04							
2	760.7	0.15	26348.1	0.21	0.13	0.43	0.22	0.01							
3	196	8	12186.6	0.31	0.03	0.65	0.00	0.01							
4	50	7.5	1446.9	0.18	0.12	0.57		0.10							0.01
5	50	7.5	10739.7	0.00	0.05		0.02	0.01							0.92
6	94	0.3	9628.0												1
7	41.7	0.12	998.8	0.02	0.58	0.03	0.00	0.06							0.297
8	109.4	0.22	9498.2			0.06	0.68	0.01	0.13		0.09	0.01	0.02		
9	10	2.48	3848.3			0.21		0.02	0.43	0.01	0.27	0.02	0.05	0.01	
10	50.3	2.1	1563.9								0.99	0.01			
11	55.7	2.1	150.4								0.36	0.63	0.01		
12	-13	3.05	1612.2						0.999						
13	-0.3	3.05	46.7						0.38	0.62					
14	-90.1	3.05	124.8	0.01		0.89		0.07	0.03						
15	114.3	2.1	562.6				0.04				0.01		0.76	0.16	

The carbon distributions (expressed as a percentage of total input carbon) of the DBTO and IDBTO processes are depicted in Fig.5. From Fig. 5(a), it can be seen that the maximum carbon flow is the captured CO_2, accounting for about 54%. This was mainly because the combustion of syngas took place in the gasification and tar reforming units, leading to the generation of large amount of CO_2. The carbon contained in ethylene and propylene accounts for 29%. For the IDBTO process, the carbon to combustor contributes to the largest share of 30% of the total carbon input from Fig.5 (b). Similar to the DBTO process, the second largest carbon share is presented in olefins product, which accounts for 32% of the total carbon generation. Nevertheless, only 18% carbon is separated from syngas.

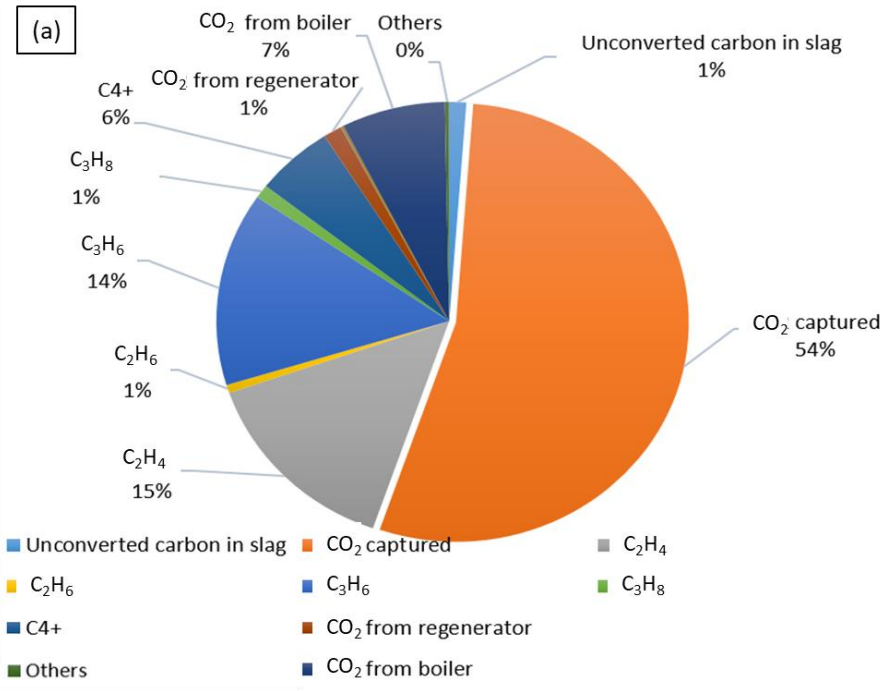

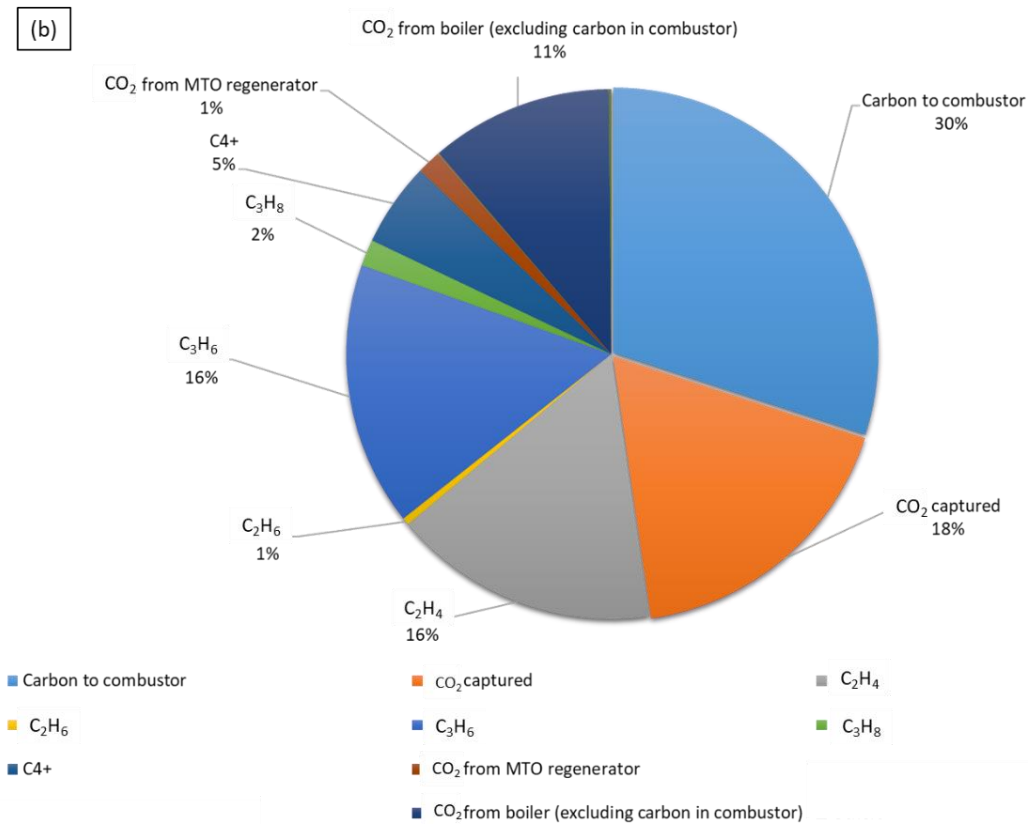

Fig.5. Carbon distribution: (a) DBTO; (b) IDBTO

4.2. Energy and exergy balance

Table 8 compares the energy balance of the two cases based on energy input, energy output and power consumption of each subsystem. It can be observed that the net power outputs of both DBTO and the IDBTO are 327.1 kW and 2612.5 kW, respectively. The larger net power output of the IDBTO can be attributed to the absence of an air separation unit. With respect to energy output of olefins, the DBTO process is about 5% lower than that of the IDBTO process. This was because of the higher olefins production yield of the IDBTO process (seeing Fig.4). As for the overall energy efficiency, it is 41.3% for the DBTO process, which is lower than that of IDBTO process (49.2%). The maximum power consumption took place in the syngas compression units for both two processes with values of 3381.7 kW and 5139.1 kW for the DBTO and IDBTO, respectively. This was mainly due to the higher flow rate

of effective syngas of the IDBTO than that of the DBTO process (as shown in Node 3 in Table 6 and 7), which resulted in additional compression power inputs.

Table 8 Energy balance of the two processes.

Item/kW	DBTO	IDBTO
Biomass input to gasifier (LHV basis)	89456.3	89456.3
Ethylene output (LHV basis)	18666.1	21112.8
Propylene output (LHV basis)	17986.3	20286.4
Power consumption		
Air separation unit	2954.9	-
O_2 compression	528.4	-
Air compression for gasification	-	401.5
Feeding and handling	575	575
Acid gas removal	413.6	194.2
CO_2 compression	640.7	195.8
Syngas compression	3381.7	5139.1
Recompression of methanol recycle gas	371.6	47.7
MTO unit	328.3	369.5
Olefins separation	157.5	178.8
Air compression for combustion	260.3	141.6
Air compression for regenerator	87.2	76.9
Pump consumption	130.1	109.1
Power generation		

High pressure steam turbine	2607.9	1818.2
Medium pressure steam turbine	3795.1	4340.9
Low pressure steam turbine	3753.4	3882.6
Net power output	327.1	2612.5
Net power efficiency/%	0.4	2.9
Overall energy efficiency/%	41.3	49.2

Exergy balance of both DBTO and the IDBTO processes is presented in Table 9. As shown in Table 9, the total exergy destruction and the loss rate are more in the DBTO as compared with the IDBTO, primarily due to the ASU (2954.9 kW) and CO_2 separation and compression unit (5059.3 kW) used in the DBTO process. Besides, the exergy destruction rate of methanol synthesis unit is higher in the DBTO than that in IDBTO. This was because of the higher RU (99%) of methanol reactor in the DBTO, leading to a higher exergy destruction compared with that of IDBTO (89%). The exergy efficiency of DBTO is presented to be 37.4 %, which is around 7% lower than that of the IDBTO.

Fig. 6 depicts exergy destruction and loss of different units against the total exergy loss for each process. It is obvious that the largest exergy destruction and loss occur in the gasification and reforming unit, which account for 48.3% and 55.6% of the total exergy loss of the DBTO and IDBTO processes, respectively. This phenomenon was mainly caused by the high irreversibility of gasification, combustion and tar reforming processes. The second largest exergy destruction and loss exists in olefins separation unit, which accounts for 10.9% and 13.3% of the total exergy loss of the DBTO and IDBTO processes, respectively. This was mainly associated with the huge amount of material losses, such as ethane, propane and C4+. At the same time, the separation of olefins via five distillation columns also led to the increase in exergy destruction due to the increase of entropy. Exergy destruction of the olefins synthesis was 5.34% for the DBTO process, while it was 7.34% for the IDBTO process.

Table 9 Exergy balance of the two processes.

Item/kW	DBTO	IDBTO
Exergy input	102788.7	102788.7
Exergy output		
Olefins	38101.6	43061.7
Power	327.1	2612.5
Exergy destruction and loss		
Air separation unit	2954.9	-
Gasification and tar reforming	31053.4	-
Gasification and steam reforming	-	31767.4
Gas cooling	1360.5	178.7
Water gas shift and water scrubber	2422.6	-
Water scrubber	-	377.3
CO_2 separation and compression	5059.3	2866.7
Methanol synthesis	2165.4	1015.4
Methanol purification	1332.3	1970.5
Methanol to olefins synthesis	3440.2	4190.2
Olefins water quench and caustic wash	1370.2	1487.5
Olefins separation	7030.7	7599.9
Purge gas combustion, HRSG, and steam turbines	6172.2	5661.2
Exergy efficiency/%	37.4	44.3

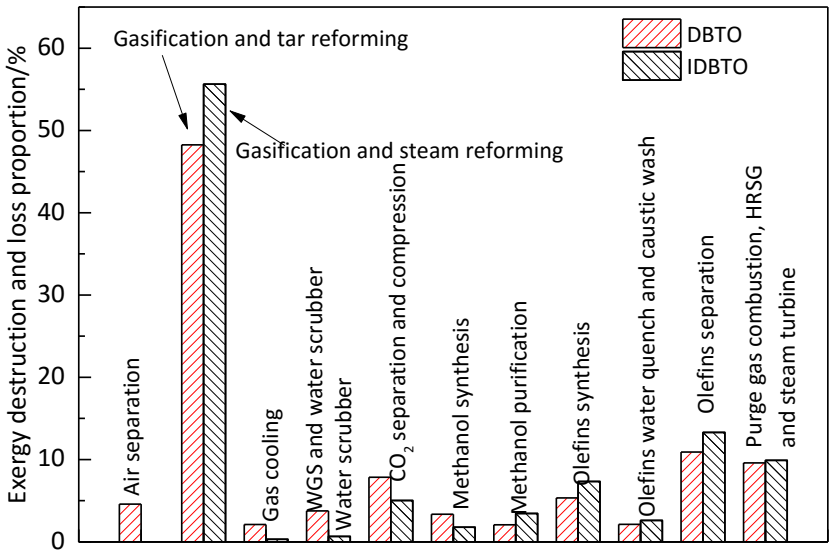

Fig.6. Exergy destruction and loss of different units in the DBTO and IDBTO processes

4.3. Sensitivity analysis

4.3.1. Effect of unreacted gas recycle fraction

The influence of RU on thermodynamic performances of the DBTO process is depicted in Fig. 7. Clearly in Fig.7 (a), an increase of the RU leads to the simultaneous increment of olefins production while the net power output decreases gently. At a RU=0.99, the olefins output reaches the maximum value of 2840.2 kg/h, whereas the net power output is shown to be the minimum value of 321.2 kW. The changes of olefins and net power output were expected since more methanol was produced as the addition of the RU, and more power was consumed to recompress the unreacted syngas. This eventually resulted in the increase in olefin yield and the reduction of net power. However, the effect of RU on the overall energy and exergy efficiencies exhibit another scenario. As shown in Fig. 7(b), when RU changes in the range of 0.2 to 0.99, the energy efficiency obviously rises from 32.5% to 41.3% and similarly, the exergy efficiency increases from 29.2% to 37.4%. It is worth noting that small increases of both efficiencies are observed when the RU exceeds 0.95. The reason of increasing system efficiencies was dominantly attributed to the addition of olefins output as seen in Fig.7 (a). However, the rapidly drop of net power

output slowed down the increase of the total energy or exergy output, leading to a small increment of both efficiencies when RU>0.95.

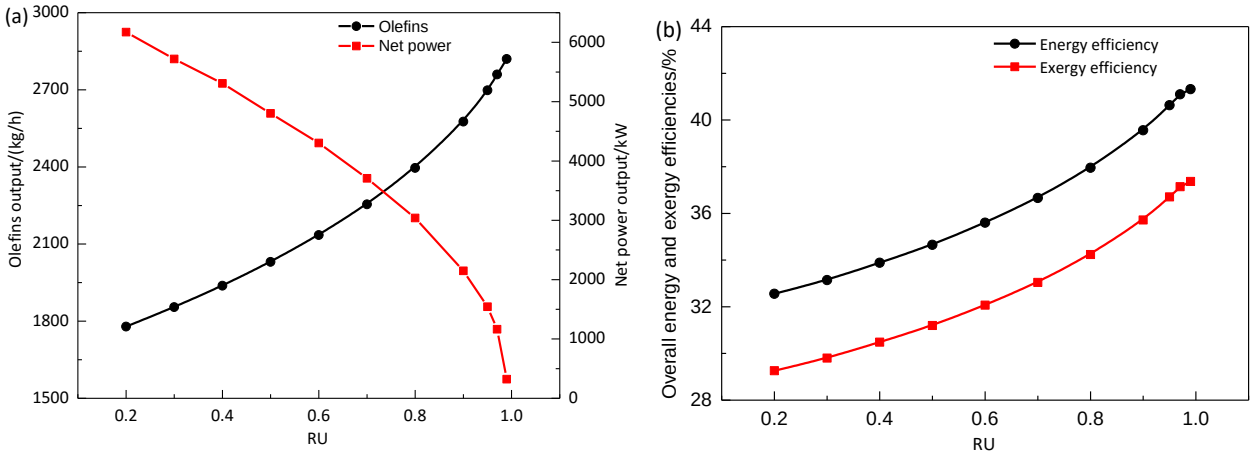

Fig.7. Effect of RU on the thermodynamic performances of DBTO process.

The effect of RU on the thermodynamic performances of the IDBTO is illustrated in Fig.8. As presented in Fig.8 (a), the olefins output increases with the addition of RU while the net power output decreased when RU is below 0.89, and levels off thereafter. From Fig. 8(b), both the energy and exergy efficiencies increase with the RU initially and then reach their maximum values (49.2% of energy efficiency and 43.3% of exergy efficiency) and drop thereafter. The initial improvement was largely because of the enhanced olefins output. As stated previously, the purge gas from methanol synthesis unit was sent to combustion to provide the energy requirement of tar reformer operating at an elevated temperature of about 800 ^{o}C. When the RU was greater than 0.89, the burning of purge gas in the tar catalyst regenerator failed to satisfy the heat demand. Thus, external fuel (such as biomass) input was required to maintain the heat balance in the tar reformer, leading to the drop of energy and exergy efficiencies significantly.

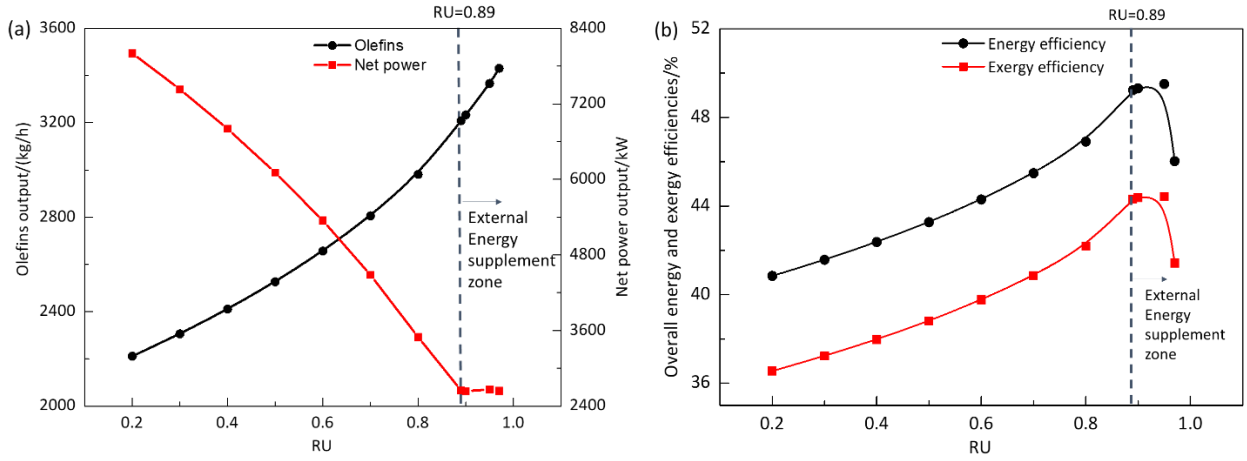

Fig.8. Effect of RU on thermodynamic performances of IDBTO process.

4.3.2. Effect of CO_2 in gasification

The effect of CO_2/B on the thermodynamic performances of the IDBTO is shown in Fig.9. Clearly in Fig. 9 (a), when CO_2/B increases from 0 to 0.185, the gasification temperature decreases promptly from 918 to 821 ºC and H_2 concentration drops slightly from 66.8 to 63.9 %, while CO concentration gradually increases from 28.9 to 30.0%. Besides, the H_2/CO molar ratio also decreases progressively from 2.31 to 2.03. The addition of CO_2 promoted the endothermic Boudouard reaction, which led to the decrease of temperature, H_2 fraction and H_2/CO molar ratio while simultaneously increased CO molar fraction. When the CO_2/B was over 0.143, external energy supplement was required. It can also be observed that the H_2/CO molar ratio of about 2.1, which suits methanol synthesis, is achieved at a CO_2/B of 0.143.

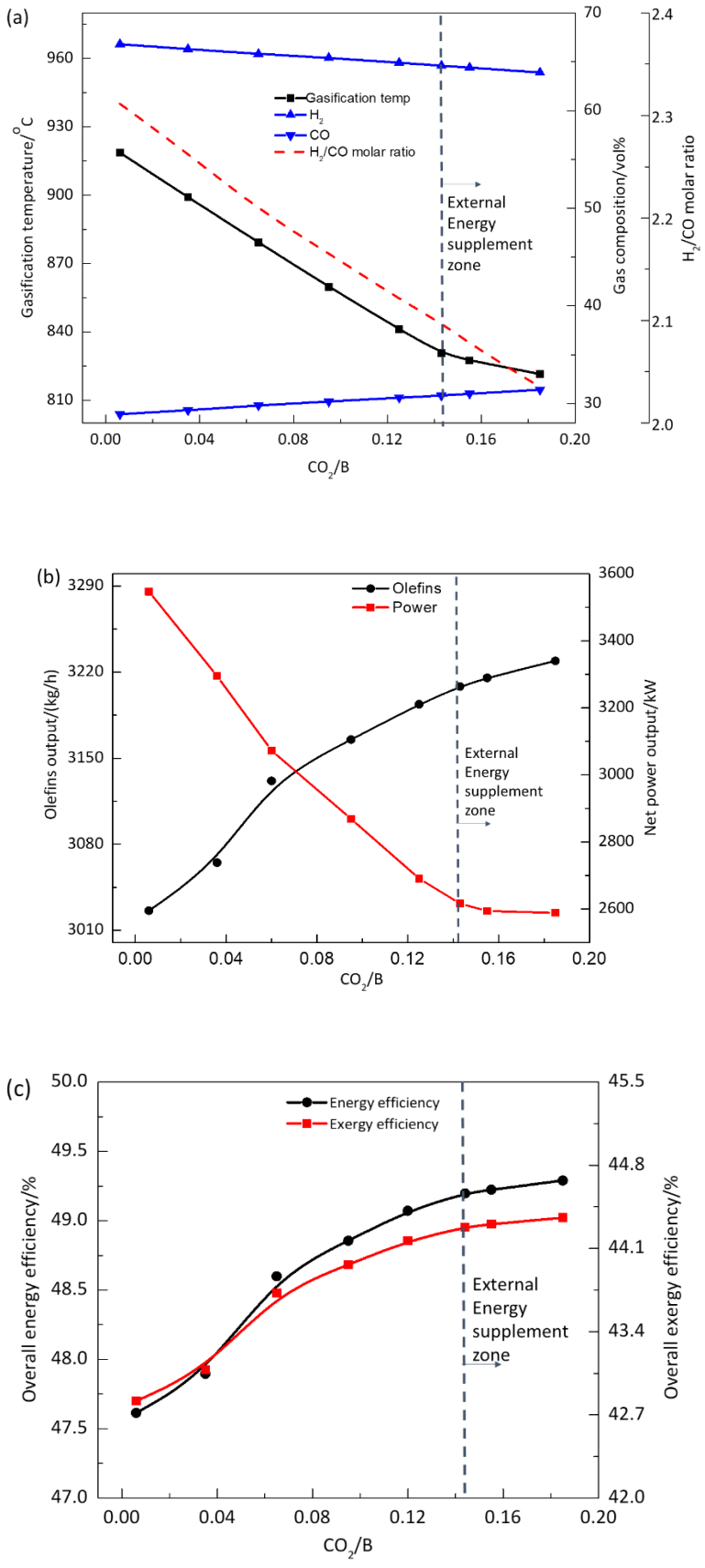

Fig.9. Effect of CO_2/B on the thermodynamic performances of IDBTO process.

The variation of olefins output and net power out with the CO_2/B is shown in Fig. 9(b). The olefins output reaches to 3229.2 kg/h, increased by 6.3% as compared with the process without CO_2 addition, whereas there is a reduction of 27% in net power output. The figure also exhibits that the upward trend of olefins and downward trend of net power are significant at the range of 0 to 0.143 and afterwards, their changing trends become small or level off. Because when the CO_2/B was beyond 0.143, the H_2/CO molar ratio was deviated the optimal ratio for the methanol synthesis gradually. As depicted in Fig.9(c), the overall energy and exergy efficiencies increase from 47.6% to 49.2% and from 42.7% to 44.3% respectively within the CO_2/B interval 0-0.143, and a slight increase is observed after that range. This was because more olefins were produced when the CO_2/B < 0.143 (shown in Fig. 9(b)), and consequently the energy and exergy efficiencies were enhanced. Nevertheless, when CO_2/B was higher than 0.143, the supplemental energy fuel was required in the combustor and it showed an increase with the addition of CO_2 input due to the endothermic Boudouard reaction. Besides, the olefins yield was shown to rise slightly as illustrated in Fig. 9(b). As a result of those combined influences, the energy and exergy efficiencies remaining steady. In summary, adjustment of the CO_2/B could achieve a desirable H_2/CO molar ratio for methanol synthesis and consequently, both the energy and exergy efficiencies increased by 1.6 % at CO_2/B=0.143 compared with no CO_2 addition scenario (CO_2/B=0).

4.4. Environmental impact evaluation

Moreover, the environmental impact evaluation was carried out to provide quantitative information of CO_2 emission via the DBTO and IDBTO routes. The results are presented in Fig.10. It is obvious that, with respect to DBTO process, the largest CO_2 emission takes place at the biomass production phase accounting for 58% of the total CO_2 positive emission, followed by the direct CO_2 emission occupying approximately 35% of the total positive CO_2 emission. However, the main contributions to CO_2 emission in the IDBTO process are direct emission and biomass production phases, with a value of 3.99 and 1.15 kg CO_2 eq./ kg olefins occupying about 76% and 22% of the total positive CO_2 emission, respectively.

The net CO_2 emissions for both processes in the entire life cycle are found to be negative. Specifically, the net CO_2 emission value of IDBTO process is - 4.44 kg CO_2 eq./ kg olefins and is - 8.74 kg CO_2 eq./ kg olefins for the DBTO. It is mainly attributed to the facts that large proportion (approx.30%, seeing Fig.5b) of residual char was forwarded to combustor for combustion to provide the heat requirement of biomass gasifier, and the resulted flue gas was emitted to the atmosphere. However, the CO_2 generated during gasification, tar reforming and WGS was captured in the DBTO process. Besides, the RU of the IDBTO process was 89% which was 10 % less than that in DBTO process. Consequently, the CO_2 emission from the combustion of purge gas for the IDBTO process was higher than that of the DBTO process. Thus, the direct and net emissions of CO_2 of IDBTO were greater than those in DBTO.

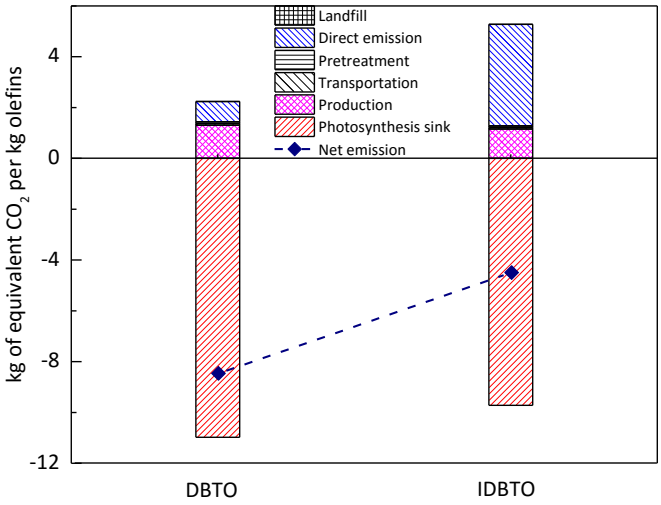

Fig.10. LCA results in CO_2 emission mass flow per kg olefins.

4.5. Economic analysis

The economic performances of the DBTO and IDBTO routes are shown in Table 10. The total capital cost of IDBTO is 74.22 M$, which is 22% lower than that of the DBTO process. This was mainly attributed to the investment elimination of an air separation unit and WGS unit in IDBTO route. Besides, the increment of equipment capital costs of MTO and methanol synthesis for IDBTO process due to higher methanol rate and syngas rate was relatively small. As a result, the total capital cost for DBTO

was higher than that of IDBTO. On the other hand, as listed in the table that the annual operating cost of DBTO is determined to 17.96 M$, which is higher than that of IDBTO about 10%. Because both processes had similar variable costs, while the fixed operating cost was calculated from proportions of total indirect capital cost, the DBTO held a higher total indirect capital cost, which led to a larger operating cost eventually.

However, the annual gross sale revenues brought by the valuable products and by-products of IDBTO system equaled to 39.62 M$·yr^{-1} and that of DBTO was calculated to be 34.30 M$·yr^{-1}. This was because more olefins and electricity were generated in the case of IDBTO. Thus, the cumulative cash flow within the plant life of IDBTO was $116.67 M higher than that of DBTO of $50.09 M, demonstrating that the IDBTO system was economically competitive. The IRR of the DBTO were 13.1 %, which is inferior to that of IDBTO with 23.5 %. Consequently, the IDBTO is more advantageous than the DBTO system in the view of economic performances.

Table 10

Economic performance of the biomass gasification to olefins processes.

Item	DBTO	IDBTO
Total capital cost, M$	96.14	74.22
Annual total operating and maintenance cost, M$/yr	17.96	16.01
Gross sale revenue, M$/yr	34.30	39.62
NPV, M$	50.09	116.67
IRR,%	13.1	23.5

To justify the impact of RU on IRR quantitatively, an economic investigation should be performed. The result is presented in Fig.11. The minimum acceptable rate of return (MARR) line of 8% is also shown in this figure. In the DBTO case, increasing RU from 0.2 to 0.99 greatly contributes to IRR from of 2.5% to 14.1%, while for the case of IDBTO, as RU enhances from 0.2 to 0.89, the IRR increases from 13.5% to 23.5% remarkably. The reason was explained as followings: increase of RU benefited olefins yield as shown in Fig.7 and Fig.8, with simultaneous promotion of gross revenues. Besides, the total capital cost decreased slightly. Consequently, the cash flow in each year was taken advantages from rising RU. The figure also implies that the RU of DBTO process should exceed to 0.65 to meet the feasibility criteria adequately.

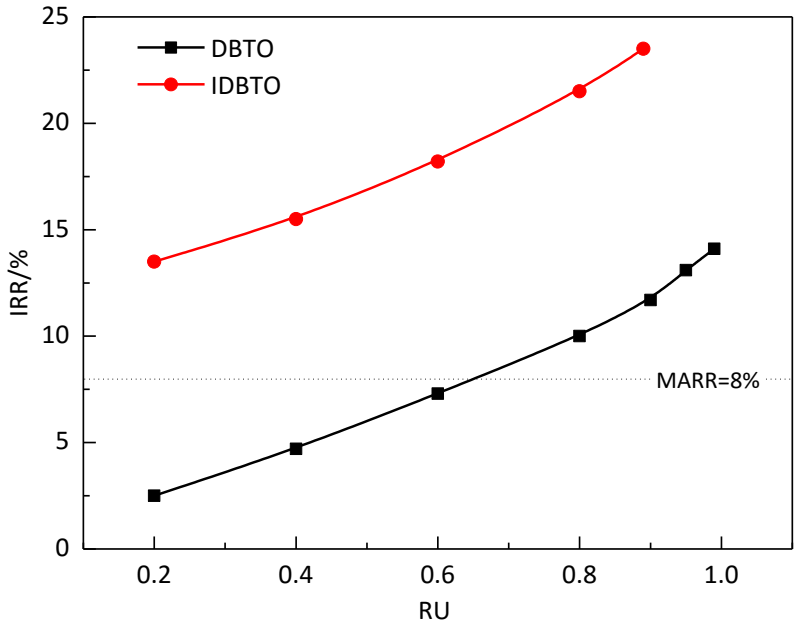

Fig.11. Effect of RU on IRR of the biomass to olefins processes

In addition, to demonstrate the economic advantages of CO_2 recycle for the IDBTO case, the effect of CO_2/B on total capital cost, gross revenue and IRR is depicted in Fig.12. The IRR exhibits increasing tendency with CO_2/B, as it rises from 22.1% to 23.5%, which reveals that the economic performance is promoted to be more profitable. The reason of increasing IRR was mainly attributed to the addition of

gross revenue introduced by the increase of olefins product (as explained previously). Clearly in Fig.12, although the total capital cost is also seen in a slight rise, its increment rate is smaller than the gross revenue, resulting from positive cash flow increase is expected. Thus, the addition of CO_2 in the IDBTO system is not only beneficial for energy and exergy efficiencies, but also it is favored financially.

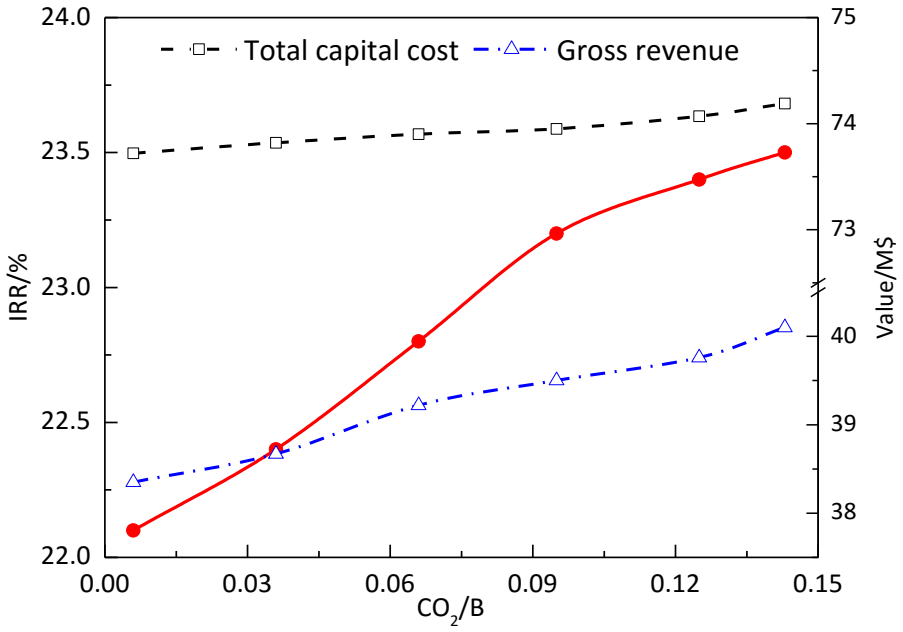

Fig.12. Effect of CO_2/B on IRR of the biomass to olefins processes

The plant capacity is another significant factor for economic assessment. Here, the variation of plant size on specific total capital cost and IRR for both processes are displayed in Fig.13 (a) and (b). With the increase of biomass feed rate to 9 kg/s, the specific total capacity cost drops about 39% for DBTO and 51% for IDBTO comparing with a 1kg/s plant, respectively. This was expected since the total equipment cost had a power law relationship with the base scale by means of Eqs.(11) [68]. Besides, the other parts in total capital cost such as buildings, site preparation, contingency, etc., were calculated from the total equipment cost. Therefore, the specific total capital cost reduced drastically followed by gradual decrease at feedstock rate of 5kg/s. In addition, since the total capital cost of IDBTO was smaller than DBTO, the effect of economy was considerably low [13]. Hence, the change in value of specific total capital cost of DBTO was less than IDBTO. However, IRR exhibits increasing tendency with plant size, as it rises from

4.3% to 16.1% for DBTO and from 9.5% to 29.1% for IDBTO, which suggests that the economic performances is enhanced. Similarly, when the plant capacity is beyond 5kg/s of feedstock rate, the IRR increasing rate slows down. It can also be noticed that the minimum profitable feedstock rate is 2.42 kg/s regarding DBTO process because the IRR exceeds 8% over that plant capacity. In contrast, the IDBTO process is profitable in the range of the studied plant size.

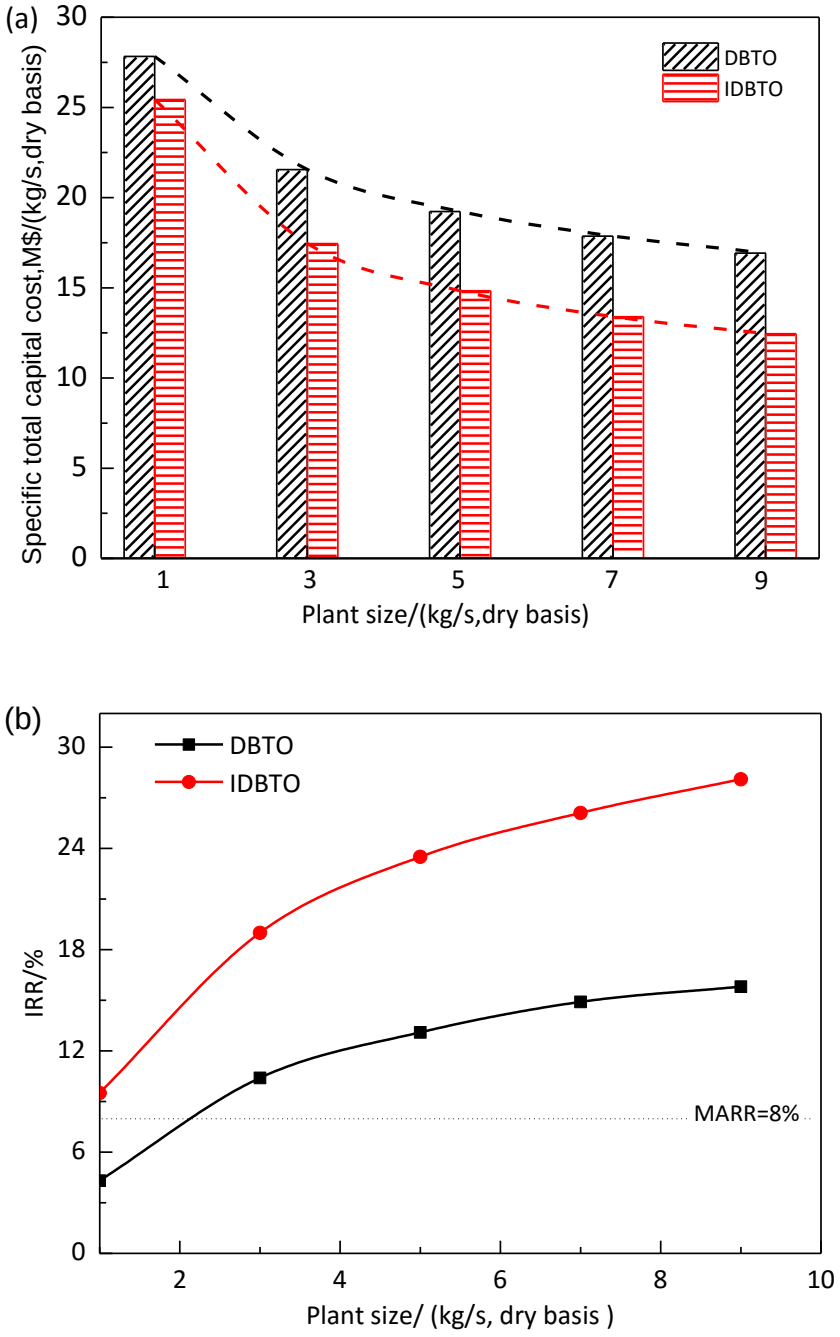

Fig.13. Effect of plant size on: (a) specific total capital cost and (b) IRR.

5. Conclusion

The indirect steam gasification of biomass to olefins via methanol as the intermediate coupled with CO_2 utilization process was proposed and compared with the direct oxygen-steam gasification of biomass to olefins process. The main findings of this study are as follows:

(1) The mass yield of olefins in DBTO was 16.9 wt%, while that of IDBTO was 19.1 wt%. The overall energy and exergy efficiencies of the IDBTO process were around 49 and 44%, respectively, compared to respective 41% and 37% in the DBTO process.

(2) The increase of RU resulted in significant improvement of overall energy and exergy efficiencies of both processes. Besides, both the energy and exergy efficiencies of the IDBTO process could be further enhanced around 1.6% when CO_2/B=0.143 compared with CO_2/B=0.

(3) The negative CO_2 emission was achieved for both processes. The IDBTO route was predicted to be -4.4 kg CO_2 eq./ kg olefins, which was 4.3 kg CO_2 eq./ kg olefins higher than that of the DBTO process.

(4) The economic evaluation indicated that the IDBTO process significantly improved economic performances as demonstrated by high NPV (116.67M$) and IRR (23.5 %).

Acknowledgement

The University of Nottingham Ningbo China is acknowledged for providing scholarship to the first author.

Reference

[1] Mei C, Wen P, Liu Z, Liu H, Wang Y, Yang W, et al. Selective production of propylene from methanol: Mesoporosity development in high silica HZSM-5. Journal of Catalysis. 2008;258(1):243-9.

[2] Hannula I, Arpiainen V. Light olefins and transport fuels from biomass residues via synthetic methanol: performance and cost analysis. Biomass Conversion and Biorefinery. 2015;5(1):63-74.
[3] Xiang D, Qian Y, Man Y, Yang S. Techno-economic analysis of the coal-to-olefins process in comparison with the oil-to-olefins process. Applied Energy. 2014;113:639-47.
[4] Chen JQ, Bozzano A, Glover B, Fuglerud T, Kvisle S. Recent advancements in ethylene and propylene production using the UOP/Hydro MTO process. Catalysis Today. 2005;106(1):103-7.
[5] Xu X, Liu Y, Zhang F, Di W, Zhang Y. Clean coal technologies in China based on methanol platform. Catalysis Today. 2017;298:61-8.
[6] Zhao Z, Liu Y, Wang F, Li X, Deng S, Xu J, et al. Life cycle assessment of primary energy demand and greenhouse gas (GHG) emissions of four propylene production pathways in China. Journal of Cleaner Production. 2017;163:285-92.
[7] Tian P, Wei Y, Ye M, Liu Z. Methanol to olefins (MTO): from fundamentals to commercialization. Acs Catalysis. 2015;5(3):1922-38.
[8] Yi Q, Zhao Y, Huang Y, Wei G, Hao Y, Feng J, et al. Life cycle energy-economic-CO 2 emissions evaluation of biomass/coal, with and without CO 2 capture and storage, in a pulverized fuel combustion power plant in the United Kingdom. Applied Energy. 2018;225:258-72.
[9] Heyne S, Thunman H, Harvey S. Exergy-based comparison of indirect and direct biomass gasification technologies within the framework of bio-SNG production. Biomass Conversion and Biorefinery. 2013;3(4):337-52.
[10] Liptow C, Tillman A-M, Janssen M. Life cycle assessment of biomass-based ethylene production in Sweden—is gasification or fermentation the environmentally preferable route? The International Journal of Life Cycle Assessment. 2015;20(5):632-44.
[11] Xiang Y, Zhou J, Lin B, Xue X, Tian X, Luo Z. Exergetic evaluation of renewable light olefins production from biomass via synthetic methanol. Applied Energy. 2015;157:499-507.
[12] Arvidsson M, Haro P, Morandin M, Harvey S. Comparative thermodynamic analysis of biomass gasification-based light olefin production using methanol or DME as the platform chemical. Chemical Engineering Research and Design. 2016;115:182-94.
[13] Xiang D, Yang S, Liu X, Mai Z, Qian Y. Techno-economic performance of the coal-to-olefins process with CCS. Chemical Engineering Journal. 2014;240:45-54.
[14] Zhou H, Qian Y, Yang S. Energetic/economic penalty of CO2 emissions and application to coal-to-olefins projects in China. Applied Energy. 2015;156:344-53.
[15] Zhang Q, Hu S, Chen D. A comparison between coal-to-olefins and oil-based ethylene in China: An economic and environmental prospective. Journal of Cleaner Production. 2017;165:1351-60.

[16] Zaini IN, Nurdiawati A, Aziz M. Cogeneration of power and H2 by steam gasification and syngas chemical looping of macroalgae. Applied Energy. 2017;207:134-45.
[17] Hannula I, Kurkela E. A parametric modelling study for pressurised steam/O2-blown fluidised-bed gasification of wood with catalytic reforming. Biomass and bioenergy. 2012;38:58-67.
[18] Zhou C, Rosén C, Engvall K. Biomass oxygen/steam gasification in a pressurized bubbling fluidized bed: Agglomeration behavior. Applied Energy. 2016;172:230-50.
[19] Mertzis D, Koufodimos G, Kavvadas I, Samaras Z. Applying modern automotive technology on small scale gasification systems for CHP production: A compact hot gas filtration system. Biomass and Bioenergy. 2017;101:9-20.
[20] Tuomi S, Kurkela E, Simell P, Reinikainen M. Behaviour of tars on the filter in high temperature filtration of biomass-based gasification gas. Fuel. 2015;139:220-31.
[21] Hsieh T-L, Zhang Y, Xu D, Wang C, Pickarts M, Chung C, et al. Chemical Looping Gasification (CLG) for Producing High Purity, H2-rich Syngas in A Co-Current Moving Bed Reducer with Coal and Methane Co-Feeds. Industrial & Engineering Chemistry Research. 2018.
[22] Hannula I, Kurkela E. A semi-empirical model for pressurised air-blown fluidised-bed gasification of biomass. Bioresource technology. 2010;101(12):4608-15.
[23] Dhanavath KN, Shah K, Bhargava SK, Bankupalli S, Parthasarathy R. Oxygen–Steam Gasification of Karanja Press Seed Cake: Fixed Bed Experiments, ASPEN Plus Process Model Development and Benchmarking with Saw Dust, Rice Husk and Sunflower Husk. Journal of Environmental Chemical Engineering. 2018;6(2):3061-9.
[24] He J, Zhang W. Techno-economic evaluation of thermo-chemical biomass-to-ethanol. Applied Energy. 2011;88(4):1224-32.
[25] Valle CR, Perales AV, Vidal-Barrero F, Gómez-Barea A. Techno-economic assessment of biomass-to-ethanol by indirect fluidized bed gasification: impact of reforming technologies and comparison with entrained flow gasification. Applied energy. 2013;109:254-66.
[26] Hannula I. Synthetic fuels and light olefins from biomass residues, carbon dioxide and electricity. Espoo: VTT Julkaisu: VTT Science. 2015;107.
[27] Azadi P, Brownbridge G, Mosbach S, Inderwildi O, Kraft M. Simulation and life cycle assessment of algae gasification process in dual fluidized bed gasifiers. Green Chemistry. 2015;17(3):1793-801.
[28] Abdelouahed L, Authier O, Mauviel G, Corriou J-P, Verdier G, Dufour A. Detailed modeling of biomass gasification in dual fluidized bed reactors under Aspen Plus. Energy & fuels. 2012;26(6):3840-55.

[29] Chaiwatanodom P, Vivanpatarakij S, Assabumrungrat S. Thermodynamic analysis of biomass gasification with CO2 recycle for synthesis gas production. Applied energy. 2014;114:10-7.
[30] Dutta A, Talmadge M, Hensley J, Worley M, Dudgeon D, Barton D, et al. Techno- economics for conversion of lignocellulosic biomass to ethanol by indirect gasification and mixed alcohol synthesis. Environmental Progress & Sustainable Energy. 2012;31(2):182-90.
[31] Fernandez-Lopez M, Pedroche J, Valverde J, Sanchez-Silva L. Simulation of the gasification of animal wastes in a dual gasifier using Aspen Plus®. Energy Conversion and Management. 2017;140:211-7.
[32] Doherty W, Reynolds A, Kennedy D. Aspen plus simulation of biomass gasification in a steam blown dual fluidised bed. 2013.
[33] Shen L, Gao Y, Xiao J. Simulation of hydrogen production from biomass gasification in interconnected fluidized beds. Biomass and Bioenergy. 2008;32(2):120-7.
[34] Proell T, Rauch R, Aichernig C, Hofbauer H. Coupling of biomass steam gasification and an SOFC-gas turbine hybrid system for highly efficient electricity generation. Conference Coupling of biomass steam gasification and an SOFC-gas turbine hybrid system for highly efficient electricity generation. American Society of Mechanical Engineers, p. 103-12.
[35] Olah GA, Goeppert A, Prakash GS. Beyond oil and gas: the methanol economy: John Wiley & Sons, 2011.
[36] Phillips SD, Tarud JK, Biddy MJ, Dutta A. Gasoline from woody biomass via thermochemical gasification, methanol synthesis, and methanol-to-gasoline technologies: A technoeconomic analysis. Industrial & engineering chemistry research. 2011;50(20):11734-45.
[37] Gong M-h, Yi Q, Huang Y, Wu G-s, Hao Y-h, Feng J, et al. Coke oven gas to methanol process integrated with CO2 recycle for high energy efficiency, economic benefits and low emissions. Energy Conversion and Management. 2017;133:318-31.
[38] Liu X, Liang J, Xiang D, Yang S, Qian Y. A proposed coal-to-methanol process with CO2 capture combined Organic Rankine Cycle (ORC) for waste heat recovery. Journal of Cleaner Production. 2016;129:53-64.
[39] Isaksson J, Pettersson K, Mahmoudkhani M, Åsblad A, Berntsson T. Integration of biomass gasification with a Scandinavian mechanical pulp and paper mill–Consequences for mass and energy balances and global CO_2 emissions. Energy. 2012;44(1):420-8.
[40] Ng KS, Sadhukhan J. Process integration and economic analysis of bio-oil platform for the production of methanol and combined heat and power. biomass and bioenergy. 2011;35(3):1153-69.

[41] Liang J, Li H, Zhao S, Guo W, Wang R, Ying M. Characteristics and performance of SAPO-34 catalyst for methanol-to-olefin conversion. Applied Catalysis. 1990;64:31-40.
[42] Xin Q, Xu J. Modern Catalysis Chemistry (in Chinese). Beijing: Science China Press, 2016.
[43] Salkuyeh YK, II TAA. Co-Production of Olefins, Fuels, and Electricity from Conventional Pipeline Gas and Shale Gas with Near-Zero CO2 Emissions. Part I: Process Development and Technical Performance. Energies. 2015;8(5):3739-61.
[44] Operation condtions and products composition of DMTO. 2011.
[45] JOHANSSON E. Process integration study of biomass-to-methanol (via gasification) and methanol-to-olefins (MTO) processes in an existing steam cracker plant: Master's thesis. Chalmers University of Technology: Gothenburg, Sweden, 2013.
[46] Fan J, Hong H, Zhu L, Jiang Q, Jin H. Thermodynamic and environmental evaluation of biomass and coal co-fuelled gasification chemical looping combustion with CO2 capture for combined cooling, heating and power production. Applied energy. 2017;195:861-76.
[47] Parvez AM, Wu T, Li S, Miles N, Mujtaba IM. Bio-DME production based on conventional and CO 2-enhanced gasification of biomass: A comparative study on exergy and environmental impacts. Biomass and Bioenergy. 2018;110:105-13.
[48] Zhang X, Li H, Liu L, Bai C, Wang S, Song Q, et al. Exergetic and exergoeconomic assessment of a novel CHP system integrating biomass partial gasification with ground source heat pump. Energy Conversion and Management. 2018;156:666-79.
[49] Corti A, Lombardi L. Biomass integrated gasification combined cycle with reduced CO2 emissions: Performance analysis and life cycle assessment (LCA). Energy. 2004;29(12-15):2109-24.
[50] Larson ED, Fiorese G, Liu G, Williams RH, Kreutz TG, Consonni S. Co-production of decarbonized synfuels and electricity from coal+ biomass with CO 2 capture and storage: an Illinois case study. Energy & Environmental Science. 2010;3(1):28-42.
[51] Beer T, Grant T, Williams D, Watson H. Fuel-cycle greenhouse gas emissions from alternative fuels in Australian heavy vehicles. Atmospheric Environment. 2002;36(4):753-63.
[52] Ng KS, Sadhukhan J. Techno-economic performance analysis of bio-oil based Fischer-Tropsch and CHP synthesis platform. Biomass and Bioenergy. 2011;35(7):3218-34.
[53] Im-orb K, Simasatitkul L, Arpornwichanop A. Techno-economic analysis of the biomass gasification and Fischer–Tropsch integrated process with off-gas recirculation. Energy. 2016;94:483-96.
[54] Albrecht FG, König DH, Baucks N, Dietrich R-U. A standardized methodology for the techno-economic evaluation of alternative fuels–A case study. Fuel. 2017;194:511-26.

[55] Kreutz TG, Larson ED, Liu G, Williams RH. Fischer-Tropsch fuels from coal and biomass. Conference Fischer-Tropsch fuels from coal and biomass, vol. 29. Princeton University Pittsburg.
[56] Onel O, Niziolek AM, Elia JA, Baliban RC, Floudas CA. Biomass and natural gas to liquid transportation fuels and olefins (BGTL+ C2_C4): process synthesis and global optimization. Industrial & Engineering Chemistry Research. 2015;54(1):359-85.
[57] Spath P, Aden A, Eggeman T, Ringer M, Wallace B, Jechura J. Biomass to hydrogen production detailed design and economics utilizing the Battelle Columbus Laboratory indirectly-heated gasifier. National Renewable Energy Lab., Golden, CO (US); 2005.
[58] Phillips SD, Tarud JK, Biddy MJ, Dutta A. Gasoline from wood via integrated gasification, synthesis, and methanol-to-gasoline technologies. National Renewable Energy Lab.(NREL), Golden, CO (United States); 2011.
[59] Liu G, Larson ED, Williams RH, Kreutz TG, Guo X. Making Fischer− Tropsch fuels and electricity from coal and biomass: performance and cost analysis. Energy & Fuels. 2010;25(1):415-37.
[60] Guangzhou Institute of Energy Conversion CAoS. Consultation on biomass power technology improvement. 2005.
[61] Huang Y, Zhao Y-j, Hao Y-h, Wei G-q, Feng J, Li W-y, et al. A feasibility analysis of distributed power plants from agricultural residues resources gasification in rural China. Biomass and Bioenergy. 2019;121:1-12.
[62] Wu H, Yu Y, Yip K. Bioslurry as a fuel. 1. Viability of a bioslurry-based bioenergy supply chain for mallee biomass in Western Australia. Energy & Fuels. 2010;24(10):5652-9.
[63] Malek AA, Hasanuzzaman M, Rahim NA, Al Turki YA. Techno-economic analysis and environmental impact assessment of a 10 MW biomass-based power plant in Malaysia. Journal of cleaner production. 2017;141:502-13.
[64] Jana K, De S. Sustainable polygeneration design and assessment through combined thermodynamic, economic and environmental analysis. Energy. 2015;91:540-55.
[65] Haro P, Johnsson F, Thunman H. Improved syngas processing for enhanced Bio-SNG production: A techno-economic assessment. Energy. 2016;101:380-9.
[66] Xiang D, Yang S, Qian Y. Techno-economic analysis and comparison of coal based olefins processes. Energy Conversion and Management. 2016;110:33-41.
[67] Ozonoh M, Aniokete T, Oboirien B, Daramola M. Techno-economic analysis of electricity and heat production by co-gasification of coal, biomass and waste tyre in South Africa. Journal of cleaner production. 2018;201:192-206.

[68] Leboreiro J, Hilaly AK. Biomass transportation model and optimum plant size for the production of ethanol. Bioresource Technology. 2011;102(3):2712-23.